

*25th DoD Explosive Safety Seminar
Anaheim, California
18-20 August 1992*

COMPARISON OF DEBRIS TRAJECTORY MODELS FOR EXPLOSIVE SAFETY HAZARD ANALYSIS

*L. A. Twisdale and P. J. Vickery
Applied Research Associates, Inc.
6404 Falls of Neuse Road, Suite 200
Raleigh, NC 27615
Phone: (919) 876-0018*

INTRODUCTION

Robust prediction of the motion of debris from explosions is critical to the estimation of separation distances, fragment density, and debris lethality in explosive safety hazard analysis. Debris dispersion models have been developed and applied to many specific types of hazardous debris (ranging from masonry, concrete, structural steel elements, soil and rock ejecta, to bomb fragments). These models generally use 2-D (degree-of-freedom) or 3-DOF trajectory calculations and consider only the drag component of the aerodynamic force vector (*e.g.*, DOE/TIC-11268 [1980], Huang [1984], McCleskey [1988], Bowles and Oswald [1990]). For many debris geometries (such as plates, slender fragments, and structural elements with high slenderness ratios), drag component trajectory models underpredict maximum debris range and dispersion. In addition, if the potential for spin-stabilized motion exists, the safety distance for plate or disk shape fragments can significantly exceed that which would be predicted for random tumbling or other non-spin-stabilized motion [Twisdale, 1984].

This paper presents several topics related to explosive safety hazardous debris trajectory analysis. The scope of the paper is limited to free-flight trajectory analysis and does not include debris ricochet or ground roll models. Following a review of alternative trajectory models, key features of the random orientation (RO) 6-D model are summarized.

The RO 6-D model uses drag, lift, and side force components and randomly updates the rigid body orientation of the missile. It has been implemented in the TORMIS and TURMIS computer codes [Twisdale, *et al.*, 1978, 1979, 1981, 1984] for facility risk assessment from wind-borne debris hazards and for fragments and secondary missiles from exploding equipment. An aerodynamic library from existing databases has been developed for fourteen generic missile/debris shapes (including structural components, plates, chunky fragments, and secondary missiles from internal equipment). An analytically derived random tumbling mode drag coefficient (as a function of the axial and cross-flow coefficients) for cylindrical shapes is summarized for use with 2-D transport predictions of chunky fragments. An equation is also presented that allows an evaluation of whether or not spin-stabilized motion will occur for in-plane rotation of discs and plates. This paper concludes with RO 6-D vs. 2-D drag comparisons of free-flight debris range prediction for several secondary debris shapes.

REVIEW OF TRAJECTORY MODELS

Debris transport methodology predicts the free-flight motion of the primary fragments and secondary missiles that are generated by the explosion. A set of initial conditions are required for the trajectory analysis, including: the missile debris mass, geometry, initial translational and angular velocities, ejection angles, and missile inertial orientations.

Report Documentation Page

Form Approved
OMB No. 0704-0188

Public reporting burden for the collection of information is estimated to average 1 hour per response, including the time for reviewing instructions, searching existing data sources, gathering and maintaining the data needed, and completing and reviewing the collection of information. Send comments regarding this burden estimate or any other aspect of this collection of information, including suggestions for reducing this burden, to Washington Headquarters Services, Directorate for Information Operations and Reports, 1215 Jefferson Davis Highway, Suite 1204, Arlington VA 22202-4302. Respondents should be aware that notwithstanding any other provision of law, no person shall be subject to a penalty for failing to comply with a collection of information if it does not display a currently valid OMB control number.

1. REPORT DATE AUG 1992	2. REPORT TYPE	3. DATES COVERED 00-00-1992 to 00-00-1992			
4. TITLE AND SUBTITLE Comparison of Debris Trajectory Models for Explosive Safety Hazard Analysis		5a. CONTRACT NUMBER			
		5b. GRANT NUMBER			
		5c. PROGRAM ELEMENT NUMBER			
6. AUTHOR(S)		5d. PROJECT NUMBER			
		5e. TASK NUMBER			
		5f. WORK UNIT NUMBER			
7. PERFORMING ORGANIZATION NAME(S) AND ADDRESS(ES) Applied Research Associates, Inc., 6404 Falls of Neuse Road, Suite 200, Raleigh, NC, 27615		8. PERFORMING ORGANIZATION REPORT NUMBER			
9. SPONSORING/MONITORING AGENCY NAME(S) AND ADDRESS(ES)		10. SPONSOR/MONITOR'S ACRONYM(S)			
		11. SPONSOR/MONITOR'S REPORT NUMBER(S)			
12. DISTRIBUTION/AVAILABILITY STATEMENT Approved for public release; distribution unlimited					
13. SUPPLEMENTARY NOTES See also ADA260986, Volume III. Minutes of the Twenty-Fifth Explosives Safety Seminar Held in Anaheim, CA on 18-20 August 1992.					
14. ABSTRACT					
15. SUBJECT TERMS					
16. SECURITY CLASSIFICATION OF:			17. LIMITATION OF ABSTRACT	18. NUMBER OF PAGES	19a. NAME OF RESPONSIBLE PERSON
a. REPORT unclassified	b. ABSTRACT unclassified	c. THIS PAGE unclassified	Same as Report (SAR)	14	

Given these initial conditions, the transport methodology consists of aerodynamic models of the missile shapes, the governing dynamic and kinematic relations, and the solution scheme for the developed equations of motion. Integration of these equations yields the motion time-history of the missile, which provides the means to predict the free-flight motion, impact conditions and density, lethality, and safety distance.

Table 1 summarizes several basic transport models that are available for explosive safety debris hazard analysis. Trajectory models are most commonly distinguished by the type of motion they describe. Generally, one degree of freedom (1-D) refers to motion of a point along a line; two degree of freedom (2-D), to a point in a plane; three degree of freedom (3-D), to motion of a point in space; and six degree of freedom (6-D), to translational and rotational motion of a rigid body in space. Another distinguishing feature is the number of

aerodynamic force components, including moments, that are considered.

The simplest model in Table 1 is the 2-D (2 degree of freedom) model for a particle mass subjected only to the force of gravity. Two ordinary differential equations, which can be integrated in closed form, describe the parabolic motion of the particle within a vertical plane. This model generally is valid only for short distance trajectories within the donor facility to get impact conditions for sympathetic detonations and/or secondary debris generation. The next hierarchy of model sophistication involves the introduction of an aerodynamic drag force in the ballistic 2-D model. The advantage of this model over the no drag model is that it provides much more accurate predictions of motion, impact speed, and position. This model is valid for non-spinning spherical and chunky debris, for which lift and side forces and moments are negligible. The resulting coupled ordinary differential equations are integrated

TABLE 1. SUMMARY OF ALTERNATIVE TRANSPORT MODELS.

Features	Models				
	2-D, No Drag	2-D, Drag	3-D	RO 6-D	6-D
Parameters	g	g	g	g, v	f
Aerodynamic Forces	None	C_D	C_D	C_D, C_L, C_S	$C_D, C_L, C_S, C_l, C_m, C_p$
Equations of Motion ^a	2 ODE	2 Coupled ODE	3 Coupled ODE	3 Coupled ODE 3 Force Eq.	6 Coupled ODE
Simulation Efficiency	Analytic	High	High	Moderate	Low
Impact Speed Prediction ^b	+	~	~	Yes	Yes
Impact Position Prediction ^b	+	-	-	~	Yes
Impact Dispersion	-	-	-	~	Yes
Impact Orientation Prediction ^b	No	No	No	~	Yes
Impact Obliquity Prediction ^b	~	~	~	Yes	Yes
Impact Angular Velocity Prediction ^b	No	No	No	No	Yes

^a ODE = Ordinary Differential Equations.

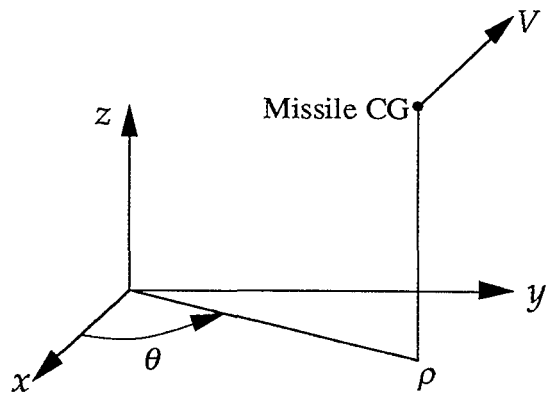
^b ~ = Approximately Correct
 - = Tendency to Underestimate
 + = Tendency to Overestimate

numerically to predict debris motion time history. The 3-D model in Table 1 predicts the general motion of a point in space. Its basic parameter is also the drag coefficient, whose value is often specified to account for random tumbling of the object. The 6-D models in Table 1 simulate the aerodynamics of rigid bodies that cannot be adequately treated by the simpler 2-D and 3-D models. The random orientation model (RO 6-D) considers drag, lift, and side forces and simulates missile tumbling by periodic reorientation [Twisdale, 1979]. Its prediction capabilities are enhanced over the particle models with only a modest decrease in simulation efficiency. Conventional 6-D models [Etkin, 1977; Redmann, *et al.*, 1978] track missile translation and rotation using a system of six coupled, ordinary, nonlinear differential equations. Such models require estimation of aerodynamic force and moment coefficients over all body orientations, which are generally not known for arbitrary bluff-body fragments.

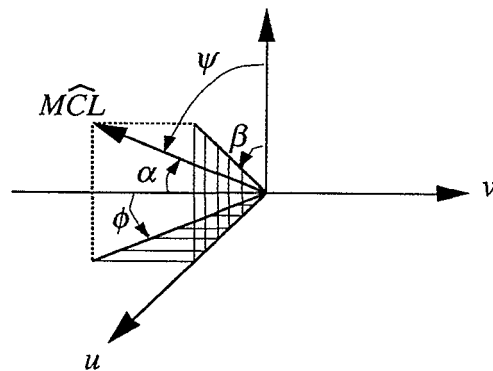
RANDOM ORIENTATION MODEL

This section presents the key features of the RO 6-D model for debris dispersion analysis, summarized from Twisdale, *et al.* [1978, 1979, 1981, 1984]. In this model, the actual rigid body orientation of the missile is considered and the aerodynamic specification includes drag, lift, and side force components. Figure 1a shows the inertial reference frame along with other reference frames that will be used in the development of the model.

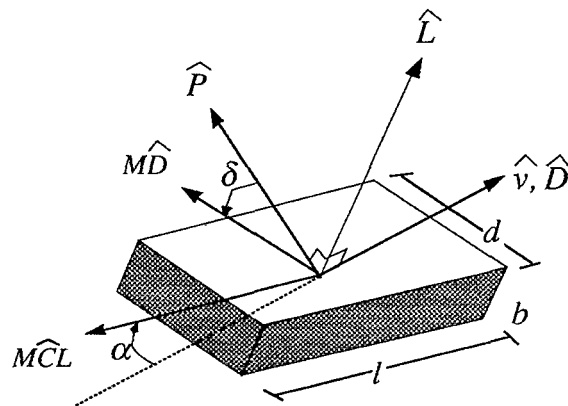
The missile centerline orientation is specified by two randomly determined angles (ψ , ϕ) measured from a (\hat{u} , \hat{v} , \hat{w}) coordinate system as defined in Figure 1b. The relative velocity vector defines the \hat{v} direction, while $\hat{u} = (\hat{v} \times \hat{k}) / |\hat{v} \times \hat{k}|$ and $\hat{w} = (\hat{u} \times \hat{v})$. Once the missile orientation is established for a time step, wind axis unit vectors are determined by forming the vector cross product of the missile centerline position unit vector (\hat{MCL})



a. Inertial Reference Frame



b. Missile Orientation



c. Relative Wind Frame

Figure 1. Coordinate Systems and Missile Specification.

with the relative velocity vector (\hat{v}) to establish the pitch axis (\hat{P}). The missile diameter unit vector ($M\hat{D}$) is rotated through a randomly selected angle (δ) from the pitch axis. The relative velocity unit vector (\hat{v}) is then combined with the pitch axis (\hat{P}) in a vector cross product to establish the lift unit vector (\hat{L}). This approach defines the wind axis system (\hat{v} , \hat{P} , and \hat{L}) for each time step and provides the respective directions for the three aerodynamic force components (drag, lift, and side) properly oriented for the missile attitude.

The magnitudes of the three translational forces are taken as proportional to the square of the relative velocity and to the three aerodynamic coefficients (C_D , C_S , and C_L), which may each be functions of total wind angle of attack (α) and roll angle (δ). These angles (α , δ) are both shown in Figure 1c. The missile angles, and hence vectors $M\hat{C}L$ and $M\hat{D}$, are updated at selected intervals according to

$$\begin{aligned} \psi &= \cos^{-1}(1 - 2\xi_1) & 0 < \psi \leq \pi \\ \phi &= \pi(2\xi_2 - 1) & -\pi \leq \phi < \pi \\ \alpha &= \cos^{-1}(\sin \psi \cos \phi) & 0 < \alpha \leq \pi \\ \delta &= 2\pi\xi_3 & 0 < \delta \leq 2\pi \end{aligned} \quad (1)$$

where ξ_1 , ξ_2 , and ξ_3 are random numbers selected from a uniform distribution on the unit interval. The time between missile orientation updates is termed the update period, and its reciprocal, update frequency. The angles α and δ are used as input to the aerodynamic coefficient determination. Once the three coefficients are determined, they are combined with the dynamic pressure, reference area (A), and the three appropriate wind axis unit vectors to form the total aerodynamic force for a single time step.

The mass center of the missile is tracked relative to the reference frame, according to

the standard dynamic equations of motion. These equations form a set of six coupled, nonlinear, ordinary differential equations that define an initial value problem for a set of prescribed initial conditions. Shampine's method [Shampine and Gordon, 1975] is used to integrate these equations.

MISSILE AERODYNAMICS FOR RO 6-D MODEL

Since complete aerodynamic characteristics generally do not exist for the potentially wide variety of debris shapes, a modified cross-flow theory has been applied to develop the aerodynamic coefficients for the random orientation model. This approach has been successfully used to develop the wind axis aerodynamic forces as a function of angle of attack for slender cylinders knowing only the drag force coefficients for the body in normal flow to the major body axes [Hoerner, 1965].

The basic theory assumes the superposition of two flows perpendicular to the missile axis (axial and cross flow) in which the magnitude of the mutually orthogonal flows is determined vectorially knowing freestream velocity and angle of attack. The aerodynamic forces acting on the missile are parallel to each flow component direction and are proportional to the directional dynamic pressure. For other shapes, flow field similarity in the cross flow regime as the angle of attack changes is the major requirement for the cross flow theory to be applicable. Thus, it is reasonable to consider extension of the theory to sharp-edged debris missiles that force boundary layer separation at a fixed point and, therefore, produce similar potential cross flow fields for all angles of attack. In principle, this concept allows the generation of lift, drag, and side forces for certain sharp-edged planar symmetric sections if the drag coefficients are known for flow normal to the three major faces of each shape. Normal flow coefficients can be found in the literature for a variety of shapes. The final form of the equations includes an aspect ratio (tip loss)

correction for finite missile dimensions, and missile face porosity. Table 2 illustrates the form of the equations for a rectangular parallelepiped shape. Figure 2 compares the cross-flow predicted lift coefficients for various roll angles to wind tunnel data for a parallelepiped missile. Summary equations for fourteen basic shapes are given in Twisdale, *et al.* [1981].

RANDOM TUMBLING MODE DRAG COEFFICIENTS

Most debris shapes are not aerodynamically stable and may exhibit autorotation, flat rotation, random tumbling, coning, or other motions during flight. These motions are governed by the initial conditions, the equations of motion, and the resulting aerodynamic and non-aerodynamic forces acting on the missile. Randomizing types of forces may arise from turbulence and non-ideal gas flows, explosive products, and missile interactions, such as debris-debris, debris-structure, and debris-ground impacts. Hence, random tumbling motion drag trajectory coefficients are often used in 2-D and 3-D drag models to predict motion of irregular, bluff body shapes and fragments. Because of the differences in the random tumbling mode (RTM) coefficients presented in the literature (*e.g.*, Bates and Swanson [1967] and Redmann, *et al.* [1976]), a validated equation is summarized herein. Use of RTM coefficients in 2-D or 3-D drag models should be used only to get the approximate center of the impact dispersion pattern and not to estimate the debris dispersion or safety distance.

The expression for the expected value of the drag coefficient, \bar{C}_d , of a tumbling missile is

$$\bar{C}_d = \int_0^{2\pi} \int_0^{2\pi} \int_0^{2\pi} C_d(\alpha, \beta, \delta) f(\alpha, \beta, \delta) d\delta d\beta d\alpha \quad (2)$$

where α , β , and δ are orientation angles as specified in Figure 1, and $f(\alpha, \beta, \delta)$ is the joint probability density function describing orientation likelihood. For a cylinder of diameter d and length L , cross-flow theory indicates that

$$\begin{aligned} C_d(\alpha, \beta, \delta) &= C_D(\alpha) \\ &= C_{Dc} \sin^3 \alpha + \frac{\pi d}{4L} C_{Da} |\cos^3 \alpha| \end{aligned} \quad (3)$$

Assuming uniformly random spatial orientation, $f(\alpha, \beta, \delta) = 1/8 \pi^2 \sin \alpha$ and the expression for the RTM coefficient is derived as

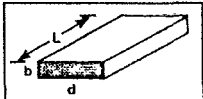
$$\bar{C}_d = \frac{1}{4} \left(\frac{3\pi}{4} C_{Dc} + \frac{\pi d}{4L} C_{Da} \right) \quad (4)$$

where the subscripts a and c refer to axial and cross-flow directions, respectively. This expression yields a significantly higher expected value than the previously published results of Bates and Swanson [1976] and Redmann, *et al.* [1976]. It is noted that this general formulation agrees with that given by Sentman and Niece [1967]. Trajectories computed using the random orientation model (drag force only) with high update frequencies are shown by Twisdale, *et al.* [1979] to converge exactly to the impact point predicted by 2-D trajectory calculations with \bar{C}_d given by Equation 4.

SPIN-STABILIZED TRAJECTORIES

The possibility of spinning flat-plate or disc-shaped fragments has been recognized in the explosive safety literature (*e.g.*, Moseley and Whitney [1980]) in terms of probable maximum debris range. High in-plane spin rates (flat rotation), imparted as a result of the explosion effects or secondary missiles from failed rotating equipment, can lead to lifting forces and significant out-of-plane trajectory motion. When these conditions exist in explosive safety problems, they should be

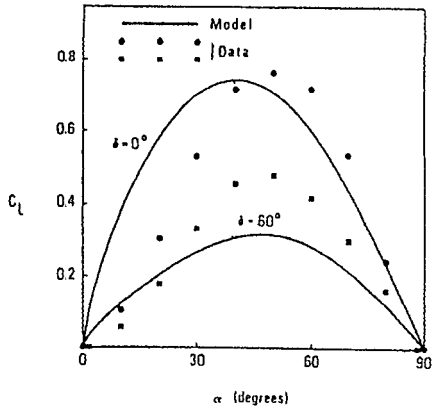
TABLE 2. CROSS FLOW AERODYNAMICS FOR PARALLELEPIPEDS.

Missile type	Box, beam, plate, frame				
Generic shape	Rectangular parallelepiped				
					
Subcategories	b/d = 1	b/d = 3	b/d = 4	b/d = 10	b/d = 50
Set nos.	5,6,18,19,20		7,8,9	10,11,21,22,23	12,13
C _{Da}	2.05 Solid 0.82 Frame/ truss	2.05 Solid	2.05 Solid	2.05 Solid 0.82 Frame/ truss	2.05 Solid
C _{Db}	2.05 Solid 0.82 Frame/ truss	2.0 Solid	2.0 Solid	2.0 Solid 0.80 Frame/ truss	2.0 Solid
C _{Dd}	2.05 Solid 0.82 Frame/ truss	1.4 Solid	1.0 Solid	1.075 Solid 0.43 Frame/ truss	1.575 Solid
Skin friction correction, f	$1, L/b < 3$ $0.41 + 0.59e^{-2(L/b-3)}, 3 < L/b < 4$ $0.46 + 0.0061 (L/h), L/b \geq 4$				
Aspect-ratio correction					
k _a	$0.59 + 0.41e^{-20b/d}$				
k _b	$0.59 + 0.41e^{-20d/L}$				
k _c	$0.59 + 0.41e^{-20b/L}$				
C _D	$(b/L) C_{Da} k_a \cos^3 \alpha + C_{Db} k_b \cos \delta \sin \alpha ^P \cos \delta \sin \alpha +$ $(b/d) C_{Dd} k_d \sin^3 \delta \sin^2 \alpha$				
C _L	$-(b/L) C_{Da} k_a \cos \alpha \cos \alpha \sin \alpha +$ $C_{Db} k_b \cos \delta \sin \alpha ^P \cos \delta \cos \alpha +$ $(b/d) C_{Dd} k_d \sin^3 \delta \sin^2 \alpha \cos \alpha$				
C _S	$C_{Db} k_b \cos \delta \cos \delta ^{P-1} \sin \delta \sin^P \alpha -$ $(b/d) C_{Dd} k_d \sin \delta \sin \delta \cos \delta \sin^2 \alpha$				
P	$0.5 + 0.15 (b/d) + 1.35 (b/d)^2$				
Ref. area, A	dL				

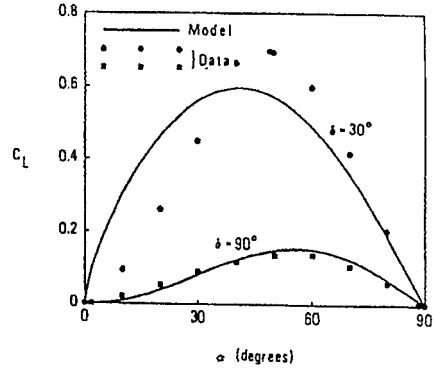
considered since they will influence the safety distance. A procedure to determine if the initial in-plane rotation rate is sufficient to stabilize a plate or disk-shaped fragment is summarized herein from the work of Twisdale, *et al.* [1984].

For purposes of developing the governing equations, a circular disc geometry is assumed. Coupling between the resultant aerodynamic force vector and the gyroscopic angular momentum vector will cause the spinning disc to slowly precess about an axis perpendicular to the spin axis. The minimal

rotational speed required to maintain this spin stabilized motion and the resulting precessional rate is developed for a symmetric disk rotating about its center of gravity. The disc sector rotates about an axis parallel to the Y-axis and passing through the center of gravity. Referring to Figure 3, let the Y-axis of the rotating reference system lie along the axis of the disk. Let this axis make an angle θ with a fixed vertical axis OB, and let it precess at a rate Ω about OB. The X-axis is in the horizontal plane AOC and is

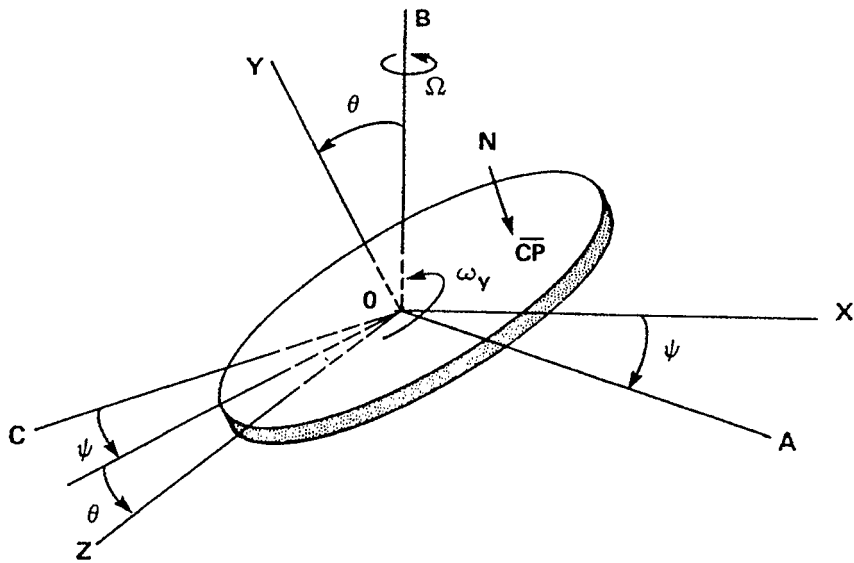


a. Lift Coefficients for $\delta = 0^\circ, 60^\circ$

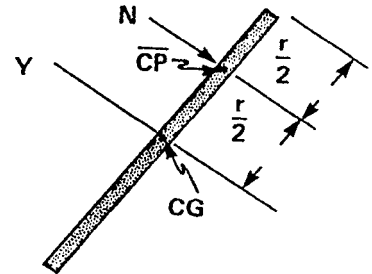


b. Lift Coefficients for $\delta = 30^\circ, 90^\circ$

Figure 2. Comparison of Cross Flow Lift Coefficients to Wind Tunnel Data for Parallelepiped.



a. Reference Frame and Notation



b. Aerodynamic Center of Pressure

Figure 3. Conical Precession of a Disc About a Vertical Axis.

perpendicular to both OY and OB. The Z-axis, perpendicular to OY and OX, lies in the vertical plane through OB and OY. Projection of Ω on the three rotating axes thus gives

$$\Omega_x = 0; \quad \Omega_y = \Omega \cos \theta; \quad \Omega_z = \Omega \sin \theta \quad (5)$$

and, since OY coincides with the axis of the disk,

$$\omega_x = \Omega_x = 0; \quad \omega_z = \Omega_z = \Omega \sin \theta \quad (6)$$

The angular velocity ω_y of the disk about OY is an input value determined by the initial conditions.

Euler's dynamical equations of motion reduce to

$$M_x = \Omega \sin \theta (I_y \omega_y - I_z \Omega \cos \theta); \quad M_y = 0; \quad M_z = 0 \quad (7)$$

where I_y and I_z are the moments of inertia. From Equation 7, the maintenance of the assumed motion requires only a moment about the X-axis. This moment is provided by the aerodynamic force normal to the circular face of the disk acting at the center of pressure, CP (Figure 3b). Assuming for the circular disk that the center of pressure is located approximately halfway between the "leading edge" of the disc and its geometric center, the moment due to the aerodynamic forces is estimated by

$$M_x = 1/2 Nr \quad (8)$$

where N is the aerodynamic force acting normal to the plane of the disc. From Equations 7 and 8, the steady precessional motion maintained by this moment is

$$\Omega = \frac{I_y \omega_y \pm [I_y^2 \omega_y^2 - 2Nr I_z \cos \theta]^{1/2}}{2I_z \cos \theta} \quad (9)$$

Neglecting the high rate of precession corresponding to the plus sign [Rauscher,

1953], Equation 9 is evaluated from l'Hopital's rule, which leads to

$$\Omega = \frac{Nr}{2I_y \omega_y}, \quad \theta = \frac{\pi}{2} \quad (10)$$

Since the angle θ will always be less than or equal to $\pi/2$, so that $\cos \theta$ is non-negative, a steady precession (and thus a constant θ) is possible only if the rotational speed of the disk is such that the radical in Equation 9 is non-negative, i.e.,

$$\omega_y^* \geq \frac{1}{I_y} [2Nr I_z \cos \theta]^{1/2} \quad (11)$$

Equation 11 suggests that ω_y^* may be as low as zero when $\theta = 90$ degrees. However, examination of Equation 10 shows that the rate of precession corresponding to this minimum rate of spin is infinite. Thus, while mathematically there is no minimum ω_y required to spin stabilize the disc at $\theta = \pi/2$, in practice if the product $\Omega I_y \omega_y$ is not sufficient to absorb the moment $1/2 Nr$, the disc will tumble until θ becomes of sufficient magnitude that $\omega_y > \omega_y^*$, at which point the disc will become spin stabilized and will then precess at the angular velocity given by Equation 9.

Table 3 summarizes initial angular velocities, ω_y , required to stabilize several circular disk missiles for different angles of attack (α), initial velocities (v_o), and inertial orientations (θ). Three steel disks were selected with weights of 10, 100, and 1000 lbs, and radius/thickness ratios of about 10. Solutions are shown for $\alpha = 10$ and 30 degrees, $v_o = 100$ and 500 ft/sec, and $\theta = 30, 65,$ and 90 degrees. For the smaller disk (A), higher ω_y^* are required to maintain the fixed

TABLE 3. SPIN RATES REQUIRED FOR SPIN-STABILIZED TRAJECTORIES OF CIRCULAR STEEL DISKS.

Initial Conditions			ω_y^* (rpm) for Disks A, B, and C			
α (deg)	v_o (ft/sec)	θ (deg)	A wt = 10 lbs, $r = 4.7$ in thk = 0.5 in	B wt = 100 lbs, $r = 10.6$ in thk = 1.0 in	C wt = 1000 lbs, $r = 23.7$ in thk = 2.0 in	
10	100	30	54	26	12	
		65	38	18	8	
		89	8	4	2	
	500	30	270	128	60	
		65	189	89	42	
		89	38	18	9	
	30	100	30	94	44	21
			65	65	31	15
			89	13	6	3
500		30	468	221	105	
		65	327	155	73	
		89	66	31	15	

orientation than are required for the heavier disks. For all three disks, minimum spin rates are needed as $\theta \rightarrow 90^\circ$ (horizontally spinning disks). The required spin rates increase significantly as v_o is increased. These example calculations indicate that for low angles of attack, and horizontally oriented disks, less than one revolution per second (60 rpm) may stabilize > 10 lb disks traveling at less than 500 ft/sec. If spin stabilization is possible, trajectory calculations can be made using the RO 6-D model with zero update frequency for fixed inertial orientation flight.

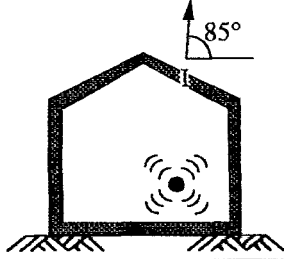
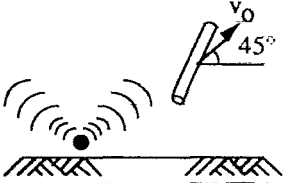
MODEL COMPARISONS AND RESULTS

The random orientation trajectory model has been developed such that it can operate in any of three modes: 3-D constant drag, random orientation with drag force only

(random drag), or random orientation, with drag, lift, and side forces (full random). Calculations with the RO 6-D model as presented for the three secondary debris missiles summarized in Table 4. The ejection angles in Table 4 are measured from the horizontal axis.

Steel Joist. In ESB Technical Paper Number 13 [DoD, 1991], the steel joist in Example Problem 1 is estimated to travel a maximum distance of 62 ft, based on a MUDEMIMP constant drag calculation. Using the RO 6-D model with drag, lift, and side force components and an update frequency of 2 hz, 100 trajectory simulations produce the impact scattergram shown in Figure 4. The initial position of the missile is $X = 0$, $Y = 0$, and the horizontal component of v_o points in the positive X direction. The range statistics are summarized in Table 5.

TABLE 4. SECONDARY MISSILE DESCRIPTIONS FOR TRAJECTORY COMPARISONS.

Parameters	Missile Description		
	1. Steel Joist	2. Steel Door	3. Secondary Fragment
			
Weight (lbs)	320	117	0.2
d (in)	8	36	0.53
L/d	20	2.33	6
V_0 (ft/sec)	111	677	985
Ejection Angle (deg)	85°	0°	45°
Reference	ESB No. 13 [DoD, 1991] Ex. Problem No. 1	ESB No. 13 [DoD, 1991] Ex. Problem No. 2	Kineke, 1976

The centroid of this scattergram is indicated by the circle. About half the trajectories travel further than the mean, and about 20% exceed the 62 ft maximum in ESB No. 13. Random tumbling flight with drag forces only has also been simulated with the RO 6-D model by using an update frequency of 100 hz. The predicted impact point is very near the centroid of the data.

Steel Door. The results for the steel door [DoD, 1991] indicate a maximum range of 808 ft. The RO 6-D scattergram for 5 hz update frequency is shown in Figure 5, and the range-to-first-impact is summarized in Table 5. The RTM-predicted range is 226 ft to first impact. These results are sensitive to update frequency with slower updates yielding larger variances in both x and y directions. Higher update frequencies

converge to RTM results with minimal variance. Note the cluster of points at about $x = 100$ ft. These indicate the position of first impact for initial orientations that result in a net downward aerodynamic force, which would cause a skid or ricochet, followed by an upward rebound of the door.

Secondary Fragment. The steel cylindrical fragment comparisons are given in Figure 6, and the statistics are summarized in Table 5 for an update frequency of 10 hz. Similar to the other missiles, the $\mu + 1\sigma$ and $\mu + 2\sigma$ distances significantly exceed the predicted RTM drag range. However, the dispersion pattern is significantly smaller, reflecting the reduced L/d over the beam missile and the higher update frequency used for this smaller fragment.

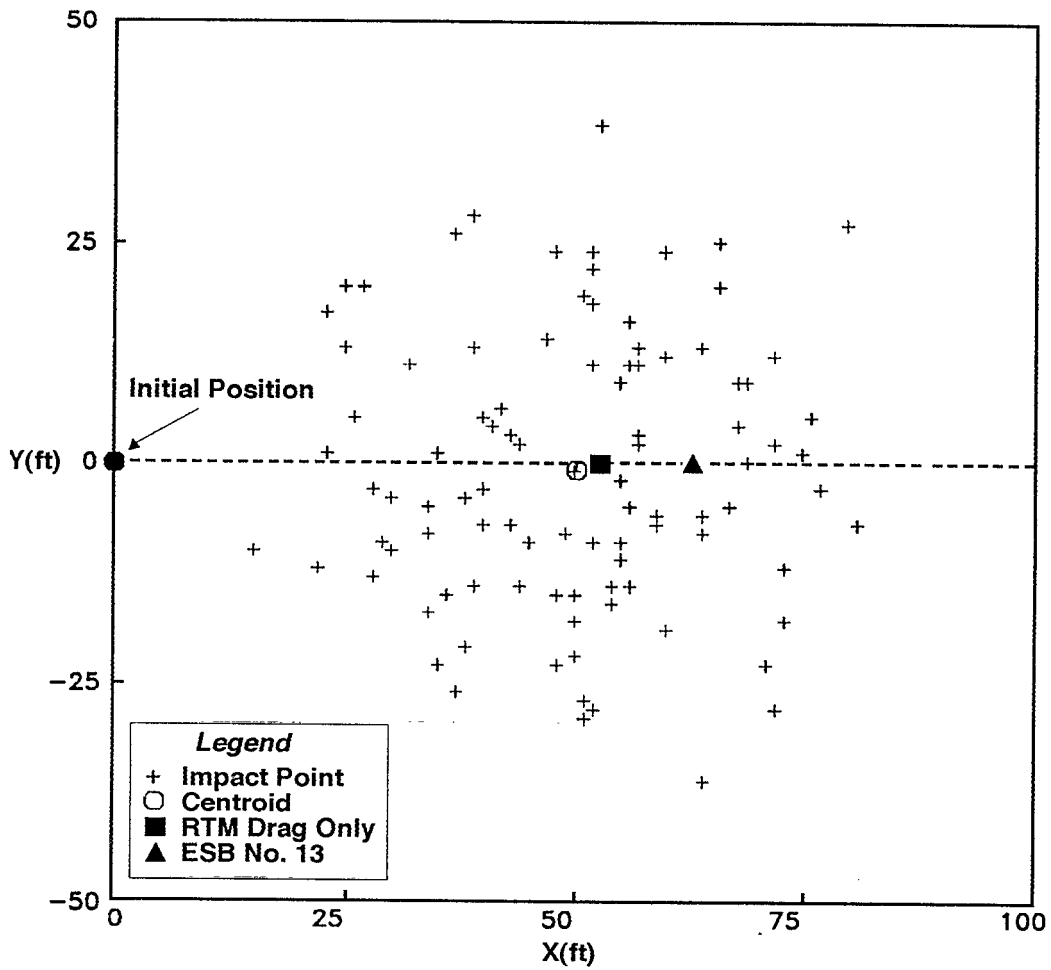


Figure 4. Impact Scattergram for Steel Joist Missile.

TABLE 5. RO 6-D TRANSPORT RANGE STATISTICS.

Missile Type	Update Frequency (hz)	2-D Drag RTM Range (ft)	RO 6-D Range Distance ¹				
			Mean (μ)	St. Dev. (σ)	$\mu + 1\sigma$	$\mu + 2\sigma$	Max
Steel Joist	2	52	52	15	67	82	84
Steel Door	5	226	495	280	775	1055	1083
Steel Fragment	10	1715	1797	121	1918	2039	2252

¹ Based on 100 simulated trajectories.

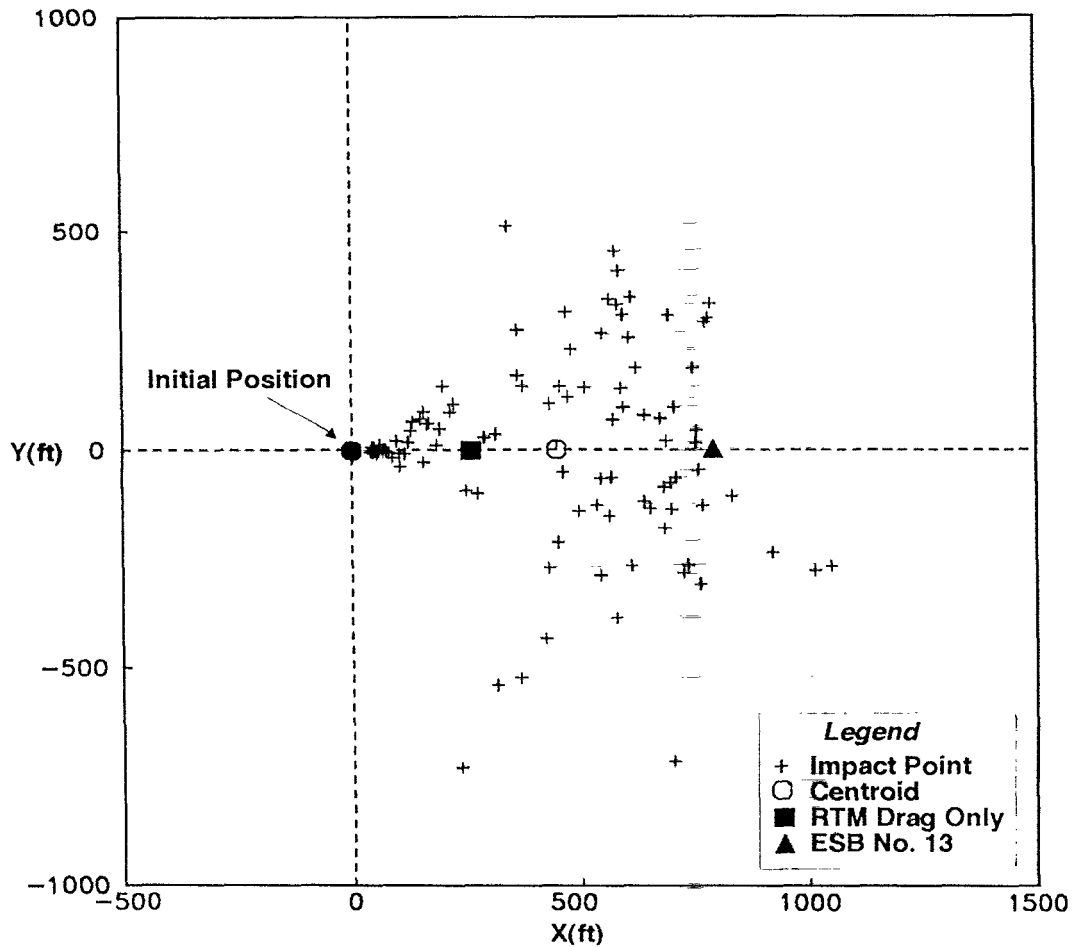


Figure 5. Impact Scattergram for Steel Door Missile.

SUMMARY

For primary fragments and secondary missiles with non-chunky shapes (plates, doors, slender fragments, and structural elements with high slenderness ratios), trajectory models that treat only the drag component of the aerodynamic force underpredict maximum debris range and dispersion. The RO 6-D model, which considers drag, lift, and side force components, provides an efficient alternative model that has been used previously in nuclear power plant missile risk assessment and to recommend debris impact velocities for the DOE NPR program. An aerodynamic

library for typical secondary missile shapes has been developed for use with the RO 6-D model. A formula for evaluating spin-stabilized flight potential for disk-shaped fragments is presented and evaluated for several disk sizes and weights.

The trajectory calculations illustrate some basic features of the RO 6-D model and the fact that maximum ranges for hazardous debris density may be underestimated by current prediction methods. The model would easily be validated for explosive safety siting analysis through a series of calculations with a full 6-D model for selected shapes, coupled

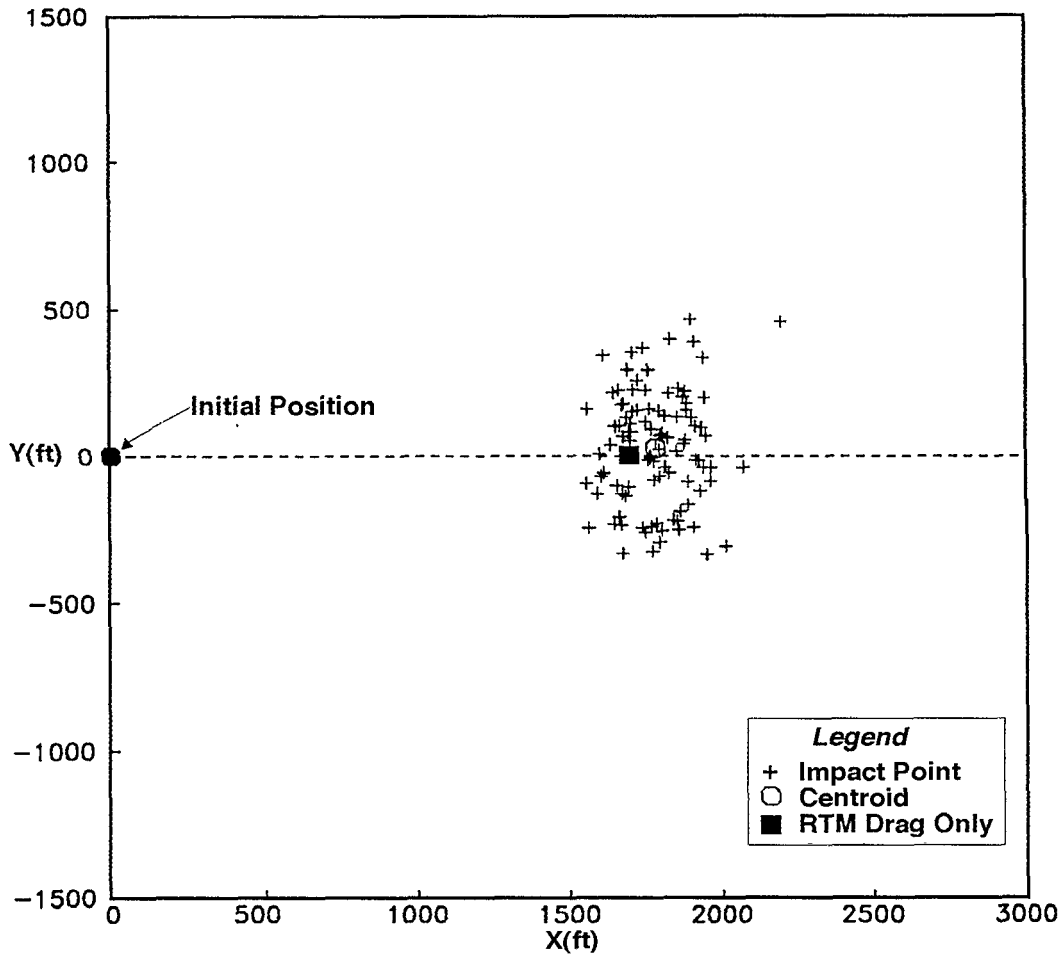


Figure 6. Impact Scattergram for Steel Cylindrical Missile.

with direct statistical analysis and comparisons to Q/D test data. The prediction methodology can efficiently simulate both chunky and non-chunky debris, and it offers several important theoretical advantages over the drag models for non-chunky shapes.

REFERENCES

Bates, E. C., and Swanson, A. E., *Tornado Design Considerations for Nuclear Power Plants*, Research Report, Black and Veach, 1976.

Bowles, P. M., and Oswald, C. J., "Building Debris Hazard Prediction Model," paper presented at the *Twenty-Fourth Department of Defense Explosives Safety Seminar*, St. Louis, Missouri, August 28-30, 1990.

Etkin, B., *Dynamics of Atmospheric Flight*, Wiley and Sons, New York, 1977.

Hoerner, S. F., *Fluid-Dynamic Drag*, published by the author, Midland Park, New Jersey, 1965.

Huang, L. C. P., *Theory and Computer Program for the Multiple Debris Missile Impact Simulation (MUDEMIMP)*, Naval Facilities Engineering Command, Naval Civil Engineering Laboratory, Program Number Y0995-01-003-331, June 1984.

McCleskey, Frank, *Quantity Distance Fragment Hazard Computer Program (FRAGHAZ)*, Naval Surface Warfare Center, TR 87-59, February 1988.

Moseley, P. K., and Whitney, M. G., "Prediction of the Blast and Debris Hazard from an Accidental Explosion in a Third Generation Norwegian Aircraft Shelter," *19th Explosive Safety Seminar*, Los Angeles, California, September 1980.

Rauscher, M., *Introduction to Aeronautical Dynamics*, Wiley and Sons, 1953.

Redmann, G. H., et al., *Wind Field and Trajectory Models for Tornado-Propelled Objects*, EPRI 308, Technical Report, Electric Power Research Institute, Palo Alto, California, February 1976.

Redmann, G. H., et al., *Wind Field and Trajectory Models for Tornado-Propelled Objects*, EPRI NP-748, Electric Power Research Institute, Palo Alto, California, May 1978.

Sentman, L. H., and Neice, S. E., "Drag Coefficients for Tumbling Satellites," *Journal of Spacecraft*, Volume 4, Number 9, September 1967.

Shampine, L. F., and Gordon, M. K., *Computer Solution of Ordinary Differential Equations: The Initial Value Problem*, W. H. Freeman, San Francisco, 1975.

Twisdale, L. A., et al., *Tornado Missile Risk Analysis*, EPRI NP-768 (Volume I) and EPRI NP-769 (Volumes I and II), Electric Power Research Institute, Palo Alto, California, May 1978.

Twisdale, L. A., Dunn, W. L., and Davis, T. L., "Tornado Missile Transport Analysis," *Journal of Nuclear Engineering and Design*, 51, 1979.

Twisdale, L. A., et al., *Tornado Missile Simulation and Design Methodology*, EPRI NP-2005, Volumes 1 and 2, Electric Power Research Institute, Palo Alto, California, August 1981.

Twisdale, L. A., Dunn, W. L., and Frank, R. A., *Probabilistic Analysis of Turbine Missile Risks*, EPRI NP-2749, Electric Power Research Institute, Palo Alto, California, January 1984.